



TiO₂-rich reconstructions of SrTiO₃(001): a theoretical study of structural patterns

Oliver Warschkow^{a,b,*}, Mark Asta^c, Natasha Erdman^c,
Kenneth R. Poeppelmeier^d, Donald E. Ellis^b, Laurence D. Marks^c

^a School of Physics, The University of Sydney, NSW 2006, Australia

^b Department of Physics and Astronomy, Northwestern University, Evanston IL, USA

^c Department of Materials Science and Engineering, Northwestern University, Evanston IL, USA

^d Department of Chemistry, Northwestern University, Evanston IL, USA

Received 16 April 2004; accepted for publication 12 October 2004

Available online 28 October 2004

Abstract

We have recently reported structure solutions for the (2×1) and $c(4 \times 2)$ reconstructions of SrTiO₃(001) based on high-resolution electron microscopy, direct methods analysis of diffraction data and density functional theory. Both reconstructions were found to be TiO₂-rich and feature a single overlayer of TiO₂ stoichiometry on top of a bulk-like TiO₂ layer. Qualitatively, the two reconstruction geometries differ in the cation sub-lattice of the overlayer only, where Ti atoms occupy half of the fivefold cation sites. In the present work we use density functional theory to generate a number of variations of this structural motif in search of patterns of stability. We find a reliable predictor for the reconstruction energy in the ability of oxygen atoms to relax vertically out of the overlayer plane to minimize non-bonded oxygen–oxygen repulsions. Out-of-plane relaxation of oxygen atoms in turn is modulated by the number and relative position of coordinating Ti atoms, which yields simple empirical rules as to how cations are distributed in low energy reconstructions.

© 2004 Elsevier B.V. All rights reserved.

Keywords: Surface structure, morphology, roughness, and topology; Surface relaxation and reconstruction; Oxygen; Density functional calculations

1. Introduction

SrTiO₃ is the quintessential perovskite and arguably, the most prominent member of an entire class of oxides that counts the lanthanum-cuprate high- T_c superconductors within its ranks. Despite

* Corresponding author. Address: School of Physics, The University of Sydney, NSW 2006, Australia. Tel.: +61 2 9036 9085; fax: +61 2 9351 7726.

E-mail address: oliver@physics.usyd.edu.au (O. Warschkow).

its bulk structural simplicity, a relatively small unit cell with high symmetry, it has an amazing number of different surface structures. For the (001) surface of SrTiO₃, a multitude of reconstruction unit cells have been observed: (1 × 1) [1], (2 × 1) [2], (2 × 2) [1,3], c(4 × 2) [4–7], c(4 × 4) [5], c(6 × 2) [4,8], (6 × 2) [8], ($\sqrt{5} \times \sqrt{5}$)R26.6° [6,9,10] and ($\sqrt{13} \times \sqrt{13}$)R33.7° [11]. The particular reconstruction formed appears to depend strongly on the experimental preparation conditions, with annealing temperature and oxygen partial pressure being the principal variables [12]. With the exception of the (2 × 1) and c(4 × 2), the atomic structure of most of the above reconstructions is unknown, owing to the general difficulties associated with oxide surface diffraction and microscopy. In the [001] direction, bulk SrTiO₃ is characterized by a stacking of layers with alternating stoichiometry TiO₂ and SrO and a number of theoretical studies have considered surfaces resulting from termination at either one of these layers

[13–18]. Non-bulk-like terminations were recently deduced for the (2 × 1) and c(4 × 2) reconstructions by way of transmission electron diffraction (TED) experiments and direct method analysis supported by density functional calculations [2,7]. This revealed that the (2 × 1) and c(4 × 2) reconstructions have an additional TiO₂-stoichiometric overlayer on top of a bulk-like TiO₂ layer (referred to in the following as the “subsurface”). As illustrated in Fig. 1, these two reconstructions are of the same stoichiometry, and differ qualitatively only in the structure of the overlayer, specifically, in the distribution of Ti cations over twice as many fivefold sites. A further characteristic is that certain oxygen atoms exhibit substantial relaxation out of the surface plane. This distinguishes the (2 × 1) and c(4 × 2) from bulk-like reconstructions and may be associated with their stability.

On simple geometric grounds, the relaxation of oxygen atoms out of the surface plane leads to surface stabilization because it reduces the repulsion

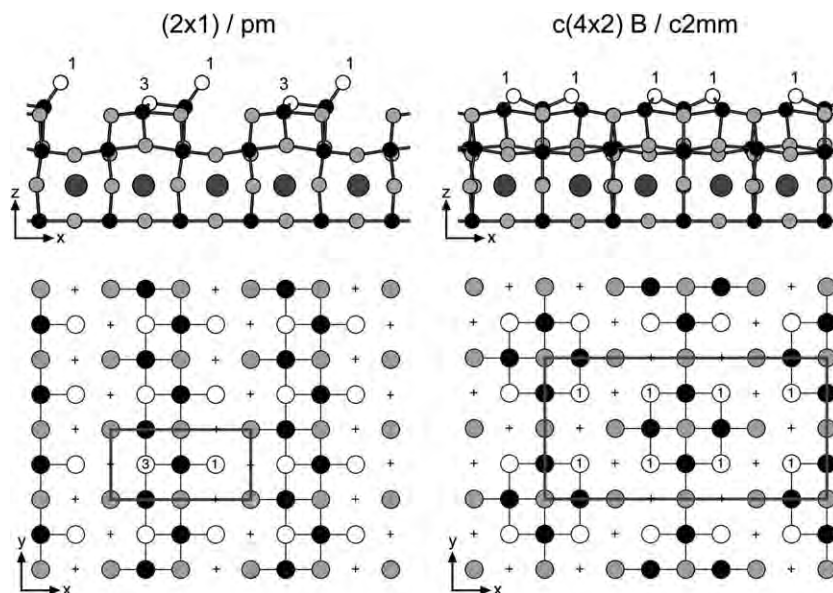


Fig. 1. Structural views of (2 × 1) and c(4 × 2) reconstructions of the SrTiO₃(001) surface as deduced from HRTEM diffraction data via direct methods analysis and density functional theory [2,7]: Ti and Sr-atoms are colored black and dark-grey (large spheres), respectively. O-atoms are colored light grey except for “floating” oxygen atoms in the TiO₂-overlayer (cf. text), which are colored white. The side-views of the surface in the upper half of the figure show how certain oxygen atoms (denoted type 1) relax out of the plane of the overlayer, while type 3 oxygen atoms are held in plane. In the lower part of the figure, the schematic top-views of the respective TiO₂-overlayer illustrate how these two reconstructions differ qualitatively in the distribution of Ti atoms (black) over available cation sites (vacant cation sites are marked with a “+”).

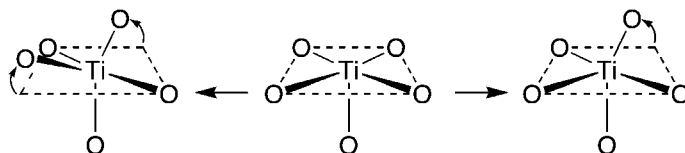


Fig. 2. Starting with a truncated octahedral coordination in an atomically flat overlayer, relaxation of oxygen atoms out of the overlayer can lead to more regular coordination polyhedra around surface bound Ti cations. This increases the distance between oxide ligands, reduces oxide–oxide repulsion and thereby stabilizes the surface.

between oxygen anions. As illustrated in Fig. 2, Ti cations in an atomically flat overlayer are coordinated in the shape of a truncated octahedron. This is not an ideal coordination geometry because the distances between oxide ligands can be increased by out-of-plane relaxation, leading to a reduction in their repulsive interactions.

In this work, we consider a number of structural variations of the observed (2×1) and $c(4 \times 2)$ reconstructions generated by density functional theory (DFT). Similar to the (2×1) and $c(4 \times 2)$, these variations are all characterized by a TiO_2 stoichiometric overlayer and differ only in the distribution of cations in the overlayer. We readily acknowledge that this represents only a subset of possible reconstructions of $\text{SrTiO}_3(001)$; however, it is only by contrasting closely related structures that qualitative insights into surface structure formation can be obtained. Here, by analyzing the variations of calculated surface energies and stresses with the distribution of the cations in the overlayer, we seek to determine “structure rules” that are of general utility and can be transferred to other perovskite oxides. As we will show below, the calculated surface energy of these TiO_2 -rich reconstructions correlates well with the out-of-plane relaxation of oxygen atoms to minimize non-bonded oxygen–oxygen repulsions. Favorable cation distributions are those that support such relaxation.

2. Computational model

Surface structures and energies reported in this work were obtained by full geometric relaxation of a 3-dimensionally periodic slab-model using first-principles density functional theory (DFT).

All calculations were performed using the ab initio total-energy and molecular-dynamics program VASP (Vienna ab initio simulation program) developed at the Institut für Materialphysik of the Universität Wien [19–22]. Calculations were performed in the generalized gradient approximation (GGA) to DFT [23,24]. Valence as well as semi-core bands (Sr-4p, Ti-3p) were expanded in a plane wave basis with a cut-off at 380 eV. Core–electron interactions were represented using Vanderbilt ultrasoft pseudopotentials [25,26]. In all of the calculations reported here the k -point mesh was taken equivalent to $4 \times 4 \times 1$ for the full (reducible) Brillouin zone corresponding to a reference (1×1) surface-unit cell [27], with the k -points shifted by $(0.5, 0.5, 0)$ away from the Γ -point. Surfaces were represented using 3D-periodic slab-models made up of seven atomic layers with the stacking sequence



mirror-symmetric about the central layer. The coordinates of all atoms in the unit cell were relaxed except for those in the central layer, which were frozen to bulk-positions. The dimensions of the simulation cell were held fixed during optimization. In the surface perpendicular direction, (i.e. $[001]$) slabs are repeated every 23.6 Å or six times the calculated bulk constant of $a = 3.937$ Å. This results in a surface-to-surface separation of approximately $3a$ (or 12 Å) through both slab and vacuum. This particular choice of slab and vacuum thickness was the result of an error analysis to minimize the effect of surface-to-surface interactions on the computed quantities of interest to this work, namely surface energy differences and stress tensor components. With a set plane wave cut-off and k -point density, available

computational resources limit the volume of the simulation cell. Because we have large surface reconstruction cells in our structural survey, up to four times the unit surface area of a (1×1) , places a limit on the $[001]$ repeat of the simulation cell; in our case $6a$ was the largest repeat at which all reconstruction geometries could be calculated. With the choice for the ratio vacuum to slab-thickness $(3a/3a)$ in the $6a$ -cell, we estimate errors due to slab and cell size effects to be below 0.04 J/m^2 for surface energy differences and below 0.5 J/m^2 for surface stress differences. These errors were estimated by comparing the results of the smaller reconstruction cells with those obtained in larger simulation cells ($[001]$ repeat up to $8a$ and up to 11 atomic layers). While these errors are certainly considerable, they are entirely acceptable for the purpose of this discussion.

3. Results

In the construction of a TiO_2 stoichiometric overlayer, the TiO_2 -stoichiometric subsurface acts in many respects as a template via bond-length constraints and the requirement for a high coordination of Ti atoms. As illustrated in Fig. 3, this suggests three types of atom sites in the overlayer:

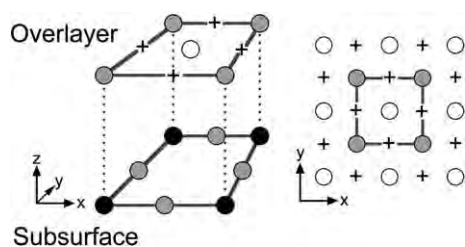


Fig. 3. Schematic perspective (left) and top-diagram (right) of possible cation and anion sites in a TiO_2 -stoichiometric overlayer formed on top of a bulk-like TiO_2 layer (the subsurface) in $\text{SrTiO}_3(001)$. “Structural” oxygen atoms (grey spheres) are positioned on top of a sub-surface Ti-atom (black). Cations sites indicated by “+” are fivefold coordinated by a single subsurface oxygen atom and in the overlayer by two structural and two floating oxygen atoms (white spheres). The latter are bound to Ti-atoms in-plane only; unlike structural oxygen atoms, they do not bind to the subsurface and have the unique ability to relax out of the surface plane.

1. “Structural” oxygen sites (grey spheres in Fig. 3) are positioned directly above Ti atoms in the sub-surfaces.
2. Titanium sites (marked by a “+” in Fig. 3) due to bond-length constraints are located between two structural oxygen sites and directly above a subsurface oxygen atom.
3. “Floating” oxygen sites (white spheres in Fig. 3) provide additional coordination to overlayer titanium atoms. Unlike “structural” oxygen atoms, they are not bound to Ti (or any other atom) in the sub-surface, which gives this site the unique ability to relax vertically out of the overlayer plane.

With the overlayer being TiO_2 stoichiometric, all oxygen sites are occupied and the only structural variable is the distribution of Ti cations over twice as many possible sites. Full DFT optimizations were performed for a number of reconstructions featuring different unit cells and distribution patterns of Ti cations. For a given unit cell, we considered a number of cation distributions, denoted as type A, B, C etc. We note that the set of distributions chosen for a given unit cell are not always complete in the sense that there may be other compatible distributions.

Schematic diagrams of all overlayer structures considered in this work are displayed in Figs. 1, 4 and 5. We have: (1×1) , (2×1) , $(\sqrt{2} \times \sqrt{2}) R45^\circ$, (2×2) , $c(4 \times 2)$ and (4×1) reconstruction unit cells. For the (1×1) reconstruction as well as the experimentally observed (2×1) , there is only one way of distributing cations in the overlayer. We include two types of $c(4 \times 2)$ reconstructions: the experimentally observed type B and what we refer to as its “subsurface isomer” type A (cf. Ref. [7]); the two subsurface isomers differ in the registry of the overlayer with respect to the bulk by a shift of $(1/2, 1/2)$. The net effect of this shift is that all “floating” and “structural” oxygen sites in the overlayer are interchanged. In addition, we have three distribution patterns for a (2×2) unit cell: A particular feature of the (2×2) C reconstruction is a structural oxygen atom that is not connected to any Ti atoms in the overlayer; this oxygen atom is only bound to a single Ti atom in the subsurface. Finally, we have

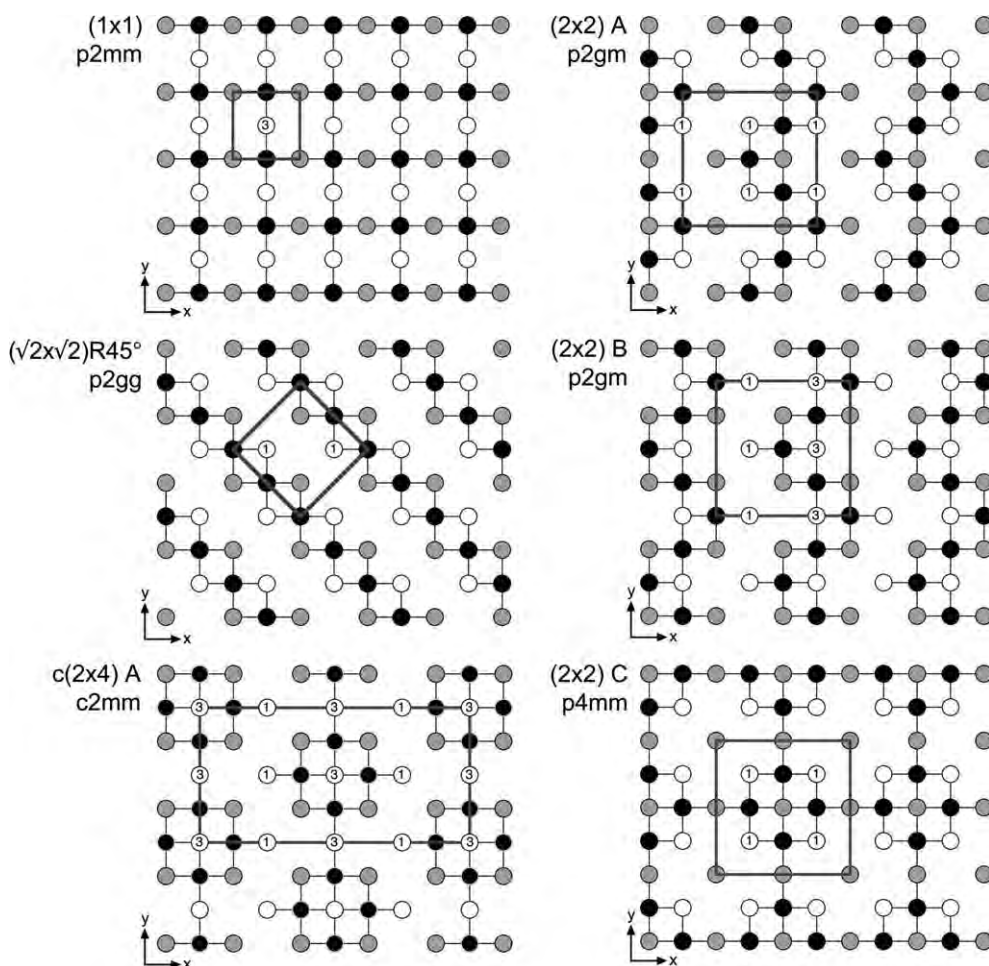


Fig. 4. Schematic top-view illustrating the cation distribution pattern for (1×1) , (2×2) type A to C, $(\sqrt{2} \times \sqrt{2})R45^\circ$ and $c(4 \times 2)$ type A reconstructions.

a single distribution pattern for a $(\sqrt{2} \times \sqrt{2})R45^\circ$ unit cell in which Ti atoms are arranged in diagonal rows, and a complete set of three distribution patterns for a (4×1) unit cell.

A topological feature of relevance to our discussion is the “connectedness” of the atoms in the overlayer. A connected network of Ti–O bonds in the overlayer defines what we refer to in the following as an “overlayer domain”. This is illustrated in Fig. 6 for the (2×1) and $(\sqrt{2} \times \sqrt{2})R45^\circ$ reconstructions, with individual domains highlighted by grey and white backgrounds. As can be seen in the figure, all the atoms within a do-

main are connected to each other through a continuous chain of Ti–O bond, whereas, no overlayer Ti–O bonds link two domains; this defines boundaries between disconnected sets of atoms. For convenience we have oriented all unit cells such that domain boundaries run along the y -direction (i.e. the bonding network is discontinuous in x); the only exception here are the (1×1) and (2×2) C, which have no boundaries, and the $(\sqrt{2} \times \sqrt{2})R45^\circ$, where the boundary is oriented at a 45° angle, i.e.; in the direction $y-x$ (cf. Fig. 4) or parallel to a $(\sqrt{2} \times \sqrt{2})R45^\circ$ unit cell vector.

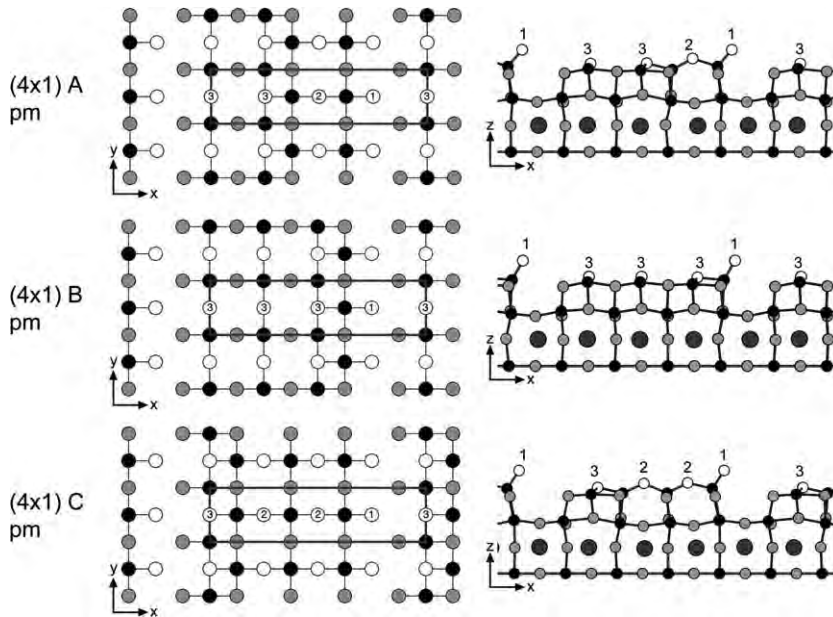


Fig. 5. Schematic top-view and structural relaxed side-view of three cation distribution patterns with (4×1) unit cell.

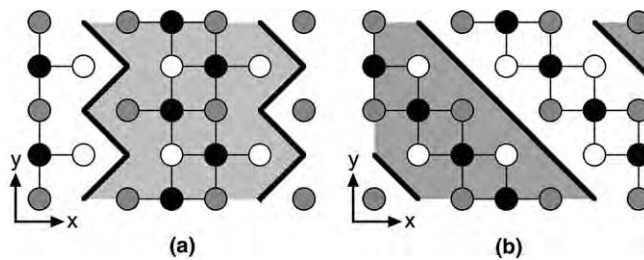


Fig. 6. Panels (a) and (b) show the schematic overlayer structure of (2×1) and $(\sqrt{2} \times \sqrt{2})R45^\circ$ reconstructions, respectively (cf. Figs. 1 and 4). Highlighted by grey and white backgrounds are separate “overlayer domains”, defined here as continuous networks of Ti–O bonds in the overlayer. Disconnected networks of atoms lead to domain boundaries, which are indicated by a thick black line. The nearest and thus strongest pair interaction across domain boundaries is between oxygen atoms (grey and white spheres) and therefore repulsive, which leads to compressive surface stresses in the direction perpendicular to the boundary.

For all reconstructions, the calculated surface energy relative to the (1×1) as well as the calculated stresses in x - and y -directions are listed in Table 1. This table also includes for reference the calculated surface stresses for two (1×1) cells terminating bulk-like at TiO_2 or SrO layers, respectively. Relative surface energies cannot be given for these two reconstructions as they are of different stoichiometry.

4. Discussion

4.1. Surface energy

On the basis of the two experimental (2×1) and $c(4 \times 2)$, reconstructions, a simple relation between cation distribution, out-of-plane relaxation and surface stability has been previously suggested [7]. Critical for the formation of regular coordination

Table 1

Calculated surface energy relative to the (1×1) reconstruction as well as surface stresses for various reconstructions of SrTiO_3 with a single TiO_2 overlayer

Unit cell	Cation pattern	F_1	F_2	F_3	Relative surface energy (J/m^2)	Stress (xx) (J/m^2)	Stress (yy) (J/m^2)
(1×1)	A	0	0	1/2	0.00	+1.1	+13.1
(2×1)	A	1/4	0	1/4	-0.10	-2.3	+4.0
$(\sqrt{2} \times \sqrt{2})R45^\circ$	A	1/2	0	0	-0.83	-2.0	-2.0
(2×2)	A	1/2	0	0	-0.69	-1.7	+0.7
	B	1/4	0	1/4	-0.17	-2.6	+1.9
	C	1/2	0	0	-0.22	+0.7	+0.7
$c(4 \times 2)$	A	1/4	0	1/4	-0.17	-3.0	-0.7
	B	1/2	0	0	-0.67	-1.3	+0.4
(4×1)	A	1/8	1/8	1/4	-0.19	-1.9	+5.5
	B	1/8	0	3/8	+0.01	-1.3	+8.6
	C	1/8	1/4	1/8	-0.47	-1.1	+3.0
Bulk-like (1×1)	TiO_2 -termin.	-	-	-	n/a	+2.4	+2.4
	SrO -termin.	-	-	-	n/a	+1.2	+1.2

Reconstructions are characterized by the unit cell, the cation distribution pattern as well as the fractions F_1 , F_2 , and F_3 of surface oxygen atoms that are “floating” of type 1, 2 and 3, respectively (cf. Figs. 1, 4, 5 and text). Positive and negative stresses are tensile and compressive; i.e., the cell seeks to contract and expand, respectively.

polyhedra around Ti, which minimize non-bonded O–O repulsion (Fig. 2), is the ability of the floating oxygen sites to relax out of plane, as this is the only atom type in the overlayer not bound to the subsurface; however, this ability is modulated by the number and relative positioning of Ti atoms in the four cation-sites nearest to the oxygen. Fig. 7 illustrates how floating oxygen atoms can relax out of the overlayer plane without Ti–O bond stretching if coordinated by only a single Ti-atom (Fig. 7a) or, alternatively, two Ti-atoms in cis-coordination (Fig. 7b). In contrast, out-of-plane relaxation is not possible in twofold-trans (Fig. 7c) as well as threefold and fourfold coordination as this would lead to bond stretching. Thus, a direct and simple correlation emerges between the cation distribution pattern and the relative stability of the reconstruction via the fraction of surface oxygen atoms that are of the floating type as well as single or twofold cis-coordinated; the larger the fraction of surface oxygen atoms that can relax out of plane, the more stable is the reconstruction.

With a larger number of reconstructions and associated surface energies in Table 1, we can now test and suitably refine this model. In Figs. 1, 4 and 5, the “floating” oxygen atoms in the reconstruction unit cell that are either single or twofold cis-coordinated are marked as type “1”, these atoms can relax freely out of the surface

plane without stretching of Ti–O bonds. Table 1 lists with the relative surface energies the fraction F_1 of overlayer oxygen atoms of this type. Fig. 8a shows graphically the correlation between F_1 and the calculated surface energy. While a general trend to lower energies with increasing F_1 is discernable, the considerable spread in the data indicates that there is more to the surface energy than merely counting type 1 oxygen sites.

As a specific example, the (2×2) C reconstruction at $F_1 = 0.5$ in Fig. 8a possesses all twofold cis-coordinated floating oxygen atoms, like the $c(4 \times 2)$ B for example. However, as is illustrated in Fig. 4, the structure of the (2×2) C reconstruction is distinct from all others in that it features structural oxygen atoms that are not coordinated by any overlayer Ti atoms; i.e.; this oxygen atom binds only to a single subsurface Ti atom. The relatively high energy of (2×2) C suggests that this must be an unfavorable structural arrangement that destabilizes the surface by a separate mechanism. We have omitted this structure from further consideration. Also noteworthy in Fig. 8a, is the relatively large spread of surface energies calculated for the three (4×1) patterns. All three (4×1) patterns contain only a single oxygen atom of type 1 thus F_1 is 1/8. Side-views of the three 4×1 reconstructions are displayed in Fig. 5. Especially for the most-stable C-reconstruction, and

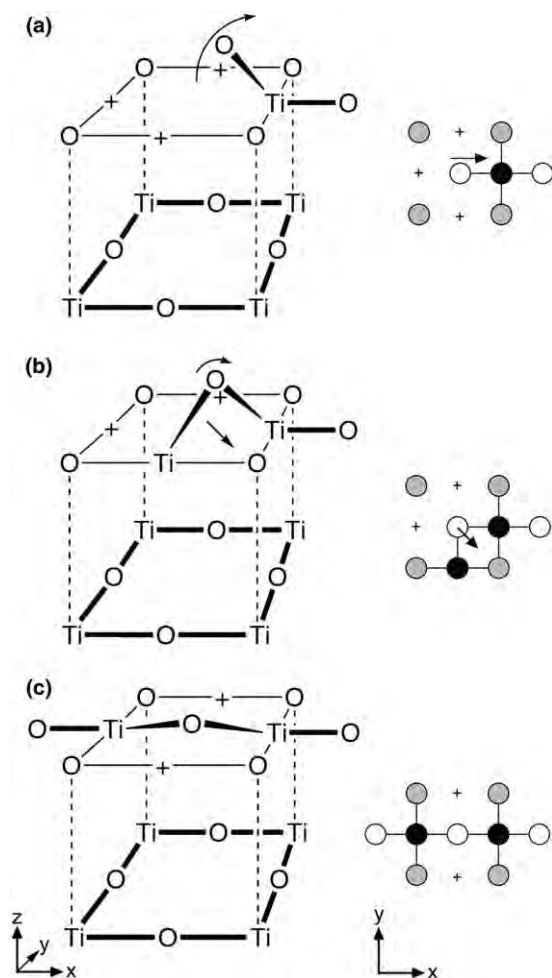


Fig. 7. Schematic perspective- (left) and top-views (right) illustrating oxygen out-of-plane relaxation as modulated by nearby cations. The ability of “floating” oxygen atoms to relax out of the overlayer depends strongly on which and how many of four nearest cation sites are occupied with Ti atoms: In single coordination (a) and twofold cis-coordination (b), the oxygen atom in the center can arc out of the surface plane without stretching Ti–O bonds. In twofold trans-coordination (c), as well as three and fourfold coordination (not shown), Ti–O bond-length constraints prevent out-of-plane relaxation of the oxygen atom.

less so for the medium stable A reconstruction, we note that some of the non-type 1 oxygen atoms are also displaced vertically out of the overlayer. These sites are marked as type 2 in the pattern diagrams. They are twofold trans-coordinated oxygen atoms and, as is evident from the structural side-

views in Fig. 5, they are able to relax out of the overlayer because the two Ti atoms they are bound to are displaced towards each other. This suggests a refinement of our model in that a twofold trans-coordinated floating oxygen atom (Fig. 7c) can relax out of plane provided that Ti atoms (and the atoms they in turn are bound to) can follow this motion. In this case bond length requirements no longer constrain the oxygen atom in the overlayer plane. We thus label in Figs. 1, 4 and 5, floating oxygen atoms as type 2 if they are twofold trans, threefold and fourfold coordinated, which can relax outwards through supporting relaxation of coordinating Ti atoms. As a general observation, we note in our reconstructions that this supporting relaxation occurs in directions perpendicular to an overlayer domain boundary (Fig. 6); evidently the discontinuity of the Ti–O bonding network provides the necessary degrees of freedom for those floating oxygen atoms trans-coordinated in this direction. We have further marked in Figs. 1, 3 and 4 all floating oxygen sites as type 3 for which out-of-plane relaxation is not possible because the coordinating Ti-atoms cannot relax in-plane to support this relaxation. These atoms are thus those that are neither of type 1 nor 2 and are held rigidly in-plane. A summary of the final classification of overlayer oxygen sites is given in Table 2. In Table 1, the fractions F_1 , F_2 and F_3 of overlayer oxygen that are of type 1, 2 and 3, respectively are listed for the various reconstructions.

Fig. 8b shows the dramatically improved correlation between surface energy and the fraction $F_1 + F_2$ of oxygen atoms that can relax out of plane.

4.2. Surface stress

Intrinsic surface stress is a measure of the degree to which the bonds near the surface are strained as a result of the constraints on their bond-lengths arising from the presence of the underlying bulk crystal structure. The correlation between calculated surface stress and the cation distribution pattern in Table 1 is less clear than was the case for the surface energies. Yet two distinct patterns emerge, related to (a) the number of

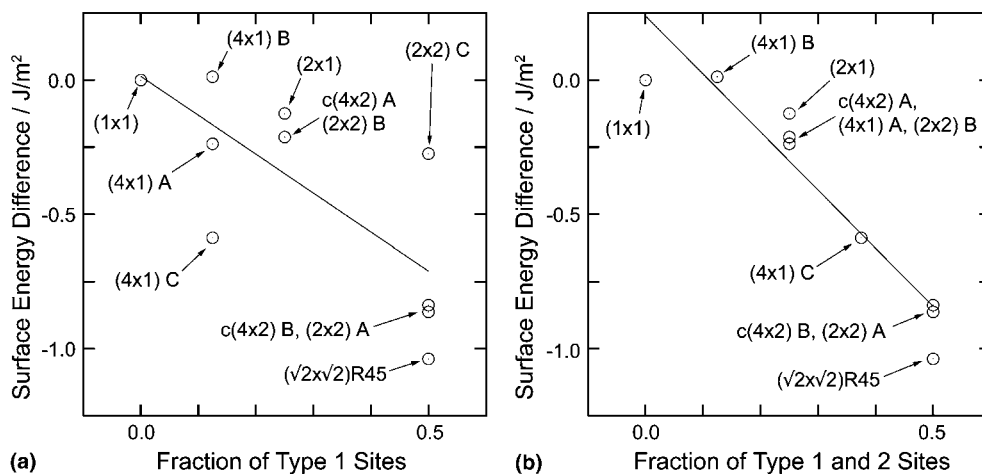


Fig. 8. Calculated relative surface energies for the set of reconstructions as a function of F_1 and $F_1 + F_2$ in panels (a) and (b), respectively. F_1 and F_2 are the fraction of overlayer oxygen atoms that are floating of type 1 and type 2, respectively.

Table 2

Summary of the four categories of oxygen sites in the overlayer, their definition and respective role as major sources of surface stabilization and stress

Oxygen type	Ti-coordination	Out-of-plane relaxation	Surface energy	Surface stress
“Structural”	Onefold to fivefold with one bond to Ti in the subsurface	Not possible due to bond to subsurface Ti atom		
“Floating”-Type 1	Onefold and twofold cis in the overlayer only	Possible	Source of stabilization	
“Floating”-Type 2	Twofold trans, threefold and fourfold in the overlayer only	Possible because coordinating atoms support out of plane relaxation	Source of stabilization	
“Floating”-Type 3	Twofold trans, threefold and fourfold in the overlayer only	Not possible. Coordinating atoms do not support out-of-plane relaxation		Source of surface stress

non-flexible (or type 3) oxygen atoms in the overlayer, and (b) boundaries between overlayer domains (Fig. 6).

Generally, we observe negative (compressive) stress in the x -direction with the (1×1) and $(2 \times 2) C$ being the only exception. This correlates directly with the fact that the (1×1) and $(2 \times 2) C$ are the only reconstructions with no overlayer domain boundaries perpendicular to the x -direction. This suggests that compressive stresses in this direction are a result of repulsion between disconnected regions of the overlayer. This is quite plausible because any such domain terminates in-plane with oxygen atoms as shown in Fig. 6; the nearest (and plausibly dominant) pair interaction across an overlayer domain boundary is between two

oxygen atoms and thus repulsive. In the $\sqrt{2} \times \sqrt{2} R45^\circ$ reconstruction, where overlayer domain boundaries run diagonally (i.e. along $[1\ 1\ 0]$) across the surface plane, the inter-domain repulsion appears as compressive stress in both in x - and y -direction.

In the y -direction, the stresses for most reconstructions are tensile, i.e. the cells generally seek to contract in this direction. Besides the $\sqrt{2} \times \sqrt{2} R45^\circ$ discussed above, the $c(4 \times 2)$ type A is the only exception. In order to rationalize the tensile stress in this direction, we focus again on the floating oxygen atoms and their ability to relax out-of-plane. Since, as shown above, these atoms are a strongly determining factor for the relative surface energy, we should expect them to contribute prom-

inently in creating surface stress, especially when it is the bulk-determined unit-cell dimensions that prevent this relaxation from taking place. We focus therefore on type 3 floating oxygen atoms that are *not* able to relax out of plane because coordinating atoms do not support their relaxation out of plane. We postulate that the inability of these oxygen atoms to relax out of plane is the dominant source of in-plane tensile stress. Remembering that type-3 floating oxygen atoms are held in plane through trans-coordination to Ti (see Fig. 7c), we can further postulate that tensile stress is created along the direction where type 3 floating oxygen atoms are trans-coordinated.

In our set of reconstructions, the largest tensile stress is created by the (1×1) reconstruction in the y -direction (Table 1). This is the direction where the only floating oxygen atom in the unit cell is trans coordinated. It is a type 3 oxygen atom since it would like to relax out-of-plane but cannot do so. For this to be possible without Ti–O bond stretching, the two trans-coordinating Ti atoms would have to relax towards each other. This in turn is only possible if the unit cell contracts along y , which is not possible because the unit cell dimensions are determined by the underlying bulk. The result is tensile surface stress in y . Comparing the three (4×1) reconstructions A to C, the calculated tensile stress in y , one finds the order $(4 \times 1) B > (4 \times 1) A > (4 \times 1) C$ which correlates with the fraction F_3 of type 3 overlayer oxygen atoms ($F_3 = 3/8, 1/4$ and $1/8$ for (4×1) patterns B, A and C, respectively). Similarly, for the three (2×2) reconstructions, the magnitude of calculated stresses in y is $(2 \times 2) B > (2 \times 2) A \approx (2 \times 2) C$ to be compared with the respective fractions F_3 of $1/4, 0$ and 0 . These comparisons suggest that there exists a correlation between the fraction of type 3 (non-flexible) floating oxygen atoms and the surface stress.

5. Conclusions

In search of structural principles guiding the formation energetics of SrTiO₃(001) surfaces, we performed DFT calculations for a number of structural variations of the experimentally observed (2×1) and $c(4 \times 2)$ reconstructions; all

characterized by a single overlayer of TiO₂ stoichiometry on top of a bulk-like TiO₂ layer and distinguished by variations in the distribution of cations over available sites. We conclude as follows:

- (1) The relative energetic stability of the reconstructions is largely controlled by the ability to displace oxygen atoms vertically out of the overlayer plane. The likely driving force behind this phenomenon is the reduction of oxide–oxide repulsion (cf. Fig. 2).
- (2) The principal actors capable of providing this stabilization are what we call “floating” oxygen atoms which are those overlayer oxygen atoms that are bound only to Ti atoms within the overlayer and not to the bulk-like layer underneath.
- (3) The number and relative placement of nearest Ti atoms limit the ability of a “floating” oxygen atom to relax out-of-plane and are thus important factors governing the stability of the surface structure. Single- and twofold-cis coordinated oxygen atoms (type 1) are free to relax out of plane without bond stretching. In contrast, twofold-trans and higher coordinated oxygen atoms can relax out-of-plane only if coordinating Ti atoms support this movement by relaxing in-plane towards each other (type 2). The fraction of surface oxygen atoms that are of either type 1 or 2 correlates well with the relative surface energy.
- (4) There is a qualitative correlation of the calculated surface stress with the fraction of floating oxygen sites that are of type 3 (i.e., neither of type 1 nor type 2). It appears that the inability of these sites to relax out of plane is a prominent source of tensile surface stress.

The results of this work point to a potentially critical role of temperature in selecting the thermodynamically stable reconstructions for SrTiO₃(001) surfaces. Specifically, we note from Fig. 8 that there are several reconstruction geometries predicted to be energetically *lower* than the observed (2×1) and $c(4 \times 2)$ B structures. It is important to emphasize that this observation does not necessarily imply that the DFT predictions are inconsistent with experiment. Specifically, the

DFT calculations yield surface energies at $T = 0$ K, whereas the experimentally observed (2×1) and $c(4 \times 2)$ structures have been prepared at 950–1000 °C and 850–930 °C, respectively [2,7]. The fact that these structures are not predicted by DFT to be amongst the lowest-energy surface phases at zero temperature suggests that thermal effects are critical in governing their observed stability. Clearly, more quantitative information are required to further clarify the nature of these thermal contributions to the relative surface stability at high temperatures; this topic will be the subject of future computational and experimental work.

Acknowledgments

This work was supported by the EMSI program of the National Science Foundation and the US Department of Energy Office of Science (CHE-9810378) at the Northwestern University Institute for Environmental Catalysis. Research of MA was supported by the NSF under program DMR-0076063.

References

- [1] B. Cord, R. Courths, Surf. Sci. 162 (1985) 34.
- [2] N. Erdman, K.R. Poeppelmeier, M. Asta, O. Warschkow, D.E. Ellis, L.D. Marks, Nature 491 (2002) 55.
- [3] Q.D. Jiang, J. Zegenhagen, Surf. Sci. 338 (1995) L882.
- [4] Q.D. Jiang, J. Zegenhagen, Surf. Sci. 425 (1999) 343.
- [5] M.R. Castell, Surf. Sci. 505 (2002) 1.
- [6] T. Matsumoto, H. Tanaka, T. Kawai, S. Kawai, Surf. Sci. 318 (1994) 29.
- [7] N. Erdman, O. Warschkow, K.R. Poeppelmeier, M. Asta, D.E. Ellis, L.D. Marks, J. Amer. Chem. Soc. 125 (2003) 10050.
- [8] M. Castell, Surf. Sci. 516 (2002) 33.
- [9] M.S. Martin-Gonzalez, M.H. Aguirre, E. Morgan, M.A. Alario-Franco, V. Perez-Dieste, J. Avila, M.C. Asensio, Solid State Sci. 2 (2000) 519.
- [10] T. Kubo, H. Nozoye, Phys. Rev. Lett. 86 (2001) 1801.
- [11] M. Naito, H. Sato, Physica C 229 (1994) 1.
- [12] N. Erdman, L.D. Marks, Surf. Sci. 526 (2003) 107.
- [13] J. Goniakowski, C. Noguera, Surf. Sci. Lett. 365 (1996) 657.
- [14] J. Padilla, D. Vanderbilt, Phys. Rev. B 56 (1997) 1625.
- [15] J. Padilla, D. Vanderbilt, Surf. Sci. 418 (1998) 64.
- [16] C. Cheng, K. Kune, M.H. Lee, Phys. Rev. B 62 (2000) 10409.
- [17] E. Heifets, R.I. Eglitis, E.A. Kotomin, J. Maier, G. Borstel, Phys. Rev. B 64 (2001) 235417.
- [18] E. Heifets, R.I. Eglitis, E.A. Kotomin, J. Maier, G. Borstel, Surf. Sci. 513 (2002) 211.
- [19] G. Kresse, J. Hafner, Phys. Rev. B 47 (1993) 558.
- [20] G. Kresse, J. Hafner, Phys. Rev. B 49 (1994) 14251.
- [21] G. Kresse, J. Furthmüller, Comput. Mater. Sci. 6 (1996) 15.
- [22] G. Kresse, J. Furthmüller, Phys. Rev. B 54 (1996) 11169.
- [23] J.P. Perdew, in: P. Ziesche, H. Eschrig (Eds.), Electronic Structure of Solids '91, Akademie Verlag, Berlin, 1991, p. 11.
- [24] J.P. Perdew, J.A. Chevary, S.H. Vosko, K.A. Jackson, M.R. Pederson, D.J. Singh, C. Fiolhais, Phys. Rev. B 46 (1992) 6671.
- [25] D. Vanderbilt, Phys. Rev. B 41 (1990) 7892.
- [26] G. Kresse, J. Hafner, J. Phys.: Condens. Matt. 6 (1994) 8245.
- [27] S. Froyen, Phys. Rev. B 39 (1989) 3168.